2007 Urban Remote Sensing Joint Event

Simulation and analysis of full-waveform laser data of urban objects

Boris JUTZI
Research Institute for Optronics and Pattern Recognition
FGAN-FOM
76275 Ettlingen, Germany
jutzi@fom.fgan.de

Uwe STILLA
Photogrammetry and Remote Sensing
Technische Universitaet Muenchen
80290 Muenchen, Germany
stilla@bv.tum.de

Abstract—**The analysis of data derived by full-waveform laser scanning systems is of great interest. In this study, we use a simulated surface response to estimate the slope of a plane surface by full-waveform analysis. For analysis the transmitted waveform of the emitted pulse is used to estimate the received waveform of the backscattered pulse for a known surface. We simulated a plane surface with different slopes. Typical spatial beam distributions are considered for modeling, namely Gaussian and uniform. The surface response is determined and the corresponding received waveform is calculated. The normalized cross-correlation function in between the estimated and the measured waveform is used to determine the slope of the surface. The similarity of the estimated and the measured received waveform is compared and discussed.**

I. INTRODUCTION

The automatic generation of 3-d models for a description of man-made objects (e.g. buildings) is of great interest. Laser systems [1] allow a direct and illumination-independent measurement of the range. They capture the range information of 3-d objects in a fast, contactless and accurate way.

Pulsed laser systems base on time-of-flight ranging techniques to determine the range of the illuminated object [12]. The time-of-flight is measured by the elapsed time between the emitted and backscattered laser pulse. The signal analysis to determine the elapsed time typically operates with analogous threshold detection. Nowadays, first pulse as well as last pulse exploitation is used for different applications (urban planning, forestry surveying) to capture a three-dimensional scene (digital terrain model, digital surface model, city model).

Beside the first or last pulse exploitation the complete waveform in between might be of interest, because it includes the backscattering characteristic of the illuminated field. This enhanced information is not only helpful to explore the vegetation concerning the bio mass, foliage or density (e.g. trees, bushes, and ground). Backscattering characteristic of urban objects can be used for estimating the aspect angle of an object plane with special surface property or estimating the surface property of a plane with a special aspect angle. This enables new techniques for reconstruction of object surfaces.

Recent developments of commercial airborne laser scanner systems led to systems that allow capturing the waveform: LITEMAPPER 5600, OPTECH ALTM 3100, TOPEYE II, and TOPOSYS HARRIER 56. The systems mentioned above are specified to operate with a transmitted pulse width of 4-10 ns and allow digitization and acquisition of the waveform with approximately 0.5-1 GSample/s.

The recording of the received waveform offers the possibility to use different methods for the range determination, e.g. peak detection, leading edge detection, centre of gravity detection, constant fraction detection. This topic was investigated by different authors, e.g. [2][4][8][9][11].

The range estimation is further improved by the comparison between the transmitted and the received waveform. This can be done by signal processing methods (e.g. cross-correlation, inverse filtering), if the sampling of the waveform is done with a high sampling rate. The maximum of the cross-correlation between the transmitted and received signal estimates the range value with a higher reliability and accuracy than considering the received waveform only [3][5][10].

Depending on the application different surfaces have to be analyzed, e.g. for urban objects we have to deal with plane objects. In rural environment we have to deal with statistically distributed natural objects. For predicting received waveforms of complex surfaces a modeling and simulation of the process is required.

The modeling of the received waveform can be done when the surface is known. A typical situation where known surfaces can be used is for registration of multiple scans received from different positions or at a different time. Beside this the surface has not to be known in advance, it can be estimated by previous measurements.

In Section II, an overview on the simulation setup with object modeling and sensor modeling is given. We show a method to calculate the surface response of a plane surface with slope in Section III. In Section IV an overview on the experimental setup is given. Assuming a plane surface with slope the corresponding received waveforms can be calculated and compared with measured waveforms, which is presented in Section V. In Section VI the method is proofed by experiments and results are depicted.

1-4244-0712-5/07/$20.00

II. Overview Of The Simulation Setup

The simulation is necessary to estimate the received waveform of the backscattered pulse from a known surface. For the transmitted waveform of the emitted pulse a measured or a modeled waveform can be used.

By the use of an object representation in form of 3-d object model (Fig. 1-1) and the extrinsic orientation parameter for sensor position and orientation (Fig. 1-2), the model is sampled to get a high-resolution range and high-reflectance image (Fig. 1-3). The resolution of these images has to be higher than the scanning grid we want to simulate for further processing. Considering the transmitted waveform of the emitted pulse and the spatial energy distribution of the laser beam for temporal and spatial laser pulse properties is relevant for modeling the laser pulse (Fig. 1-4). To simulate the spatial scanning procedure of the laser system, the values of the grid spacing and the divergence of the laser beam are used. Therefore a convolution between the high-resolution reflectance image and the spatial energy distribution of the beam (Fig. 1-5) has to be determined. For a range depending 1-d surface representation, the surface response is determined by the spatial undersampling of the high-resolution range and high-intensity image (Fig. 1-6). By convolving the surface response with the transmitted waveform the received waveform is determined at the receiver (Fig. 1-7).

For simulating the received waveform of the backscattered pulses an object model (Section II.A) and a sensor model (Section II.B) is required.

A. Object modeling

For an object representation, our simulation setup considers geometric and radiometric features of the illuminated surface in the form of 3-d object models with homogeneous surface reflectance.

The object model with homogeneous surface reflectance is then sampled higher than the scanning grid we simulate and process, because with the higher spatial resolution we simulate the spatial distribution of the laser beam. Considering the position and orientation of the sensor system we receive a high-resolution range image and high-resolution reflectance image. Depending on the predetermined position and orientation of the sensor system, various range images can be captured.

B. Sensor modeling

The sensor model takes into account the specific properties of the sensing process: the position and orientation of the sensor, the laser pulse description, the scanning process and the electrical receiver properties. To simulate various aspects, a description of the extrinsic orientation of the laser scanning system with a GPS/INS system is used.

The emitted laser pulse of the system is characterized by specific pulse properties. We assume radial symmetric uniform spatial distributions and radial symmetric Gaussian distributions for the beam profile, which are typical for the most laser systems. For this simulation we use measured transmitted waveforms to have a realistic description, where

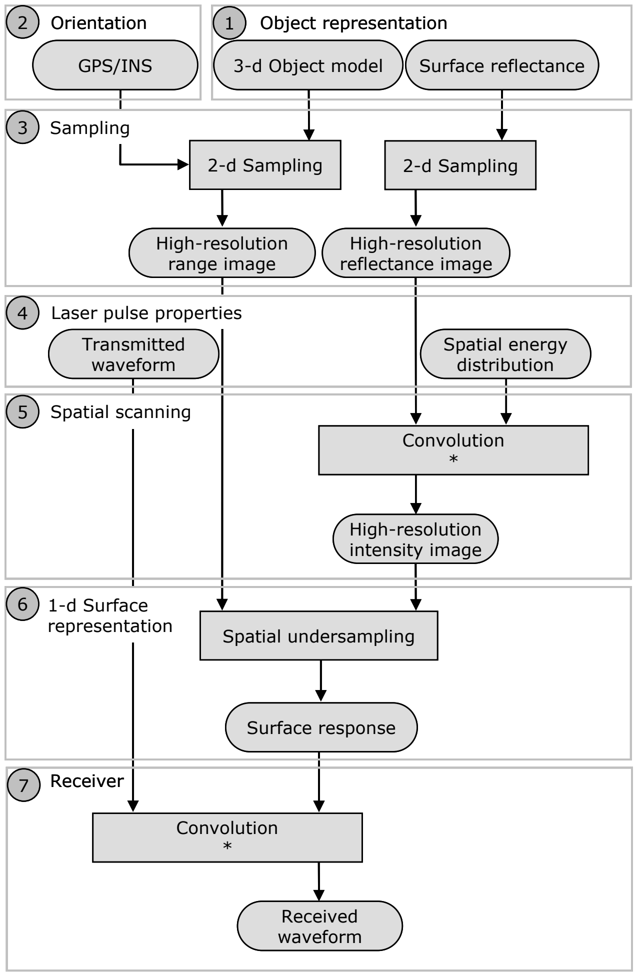

Figure 1. Simulation setup for calculating the received waveform.

the bandwidth of the receiver to capture the waveform is 6 GHz and the data is sampled with 20 GSample/s. The transmitted waveform of the used system shows strong intensity fluctuations from pulse to pulse (Fig. 2). The high sampling rate provides detailed information about the shape of the waveform with at least 100 sampling points for the typical length of the pulse (5 ns at Full-width-at-half-maximum).

Depending on the scan pattern of the laser scanner system, the grid spacing of the scanning process, and the divergence of the laser beam, a sub-area of the high-resolution range and high-resolution reflectance images is processed. Therefore, the sub-area of the high-resolution reflectance image is convolved with the spatial energy distribution of the laser beam (distribution at the grid line $\pm 2\sigma$) to take into account the amount of backscattered laser light for each reflectance value. By focusing the beam with its specific properties on the detector of the receiver, the spatial resolution is reduced and this is simulated with a spatial undersampling of the sub-areas. Therefore the received high-resolution intensity and high-resolution range image is processed by spatial undersampling to gain a weighted 1-d range distribution, which we call surface response. The determined surface response is convolved with the transmitted waveform to gain the received waveform of the backscattered pulse.

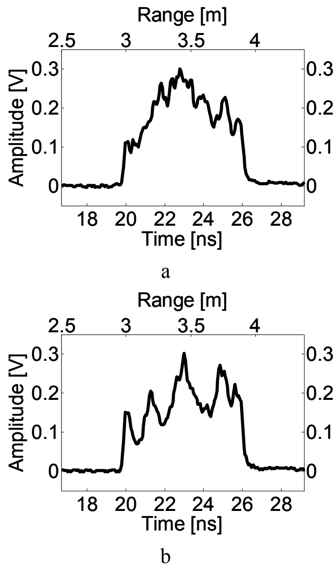

Figure 2. Samples of the transmitted waveform.

III. Calculating The Surface Response Of A Plane Surface With Slope

The received waveform of a laser pulse depends on the transmitted waveform $s[t]$, the impulse response $h[t]$ of the receiver unit, the spatial beam distribution of the used laser $P[x,y]$, and the illuminated surface $S[x,y,z]$. The received waveform $r[x,y,z,t]$ can be expressed by a convolution of the relevant terms mentioned above and we get

$$r[x,y,z,t] = s[t] * h[t] * P[x,y] * S[x,y,z]\,, \tag{1}$$

where (*) denotes the convolution operation. The impulse response is mainly effected by the used photodiode and amplifier, the spatial beam distribution has typically the shape of a Gaussian or uniform, and the surface characteristic can be described by its geometry and reflectance properties (mixture of diffuse and specular). We assume to have a receiver unit consisting out of an ideal photodiode and amplifier with an infinite bandwidth and a linear frequency characteristic. The 3-d surface characteristic can be reduced to a range depending 1-d signal $S[z]$, which we call in this paper surface response.

To study the surface response received from different surfaces, we simulated a plane surface, which can be adjusted for various slopes, illuminated by a beam with a spatial uniform beam distribution and a Gaussian beam distribution. For the simulation, the laser beam divergence is set to 1 mrad and the spatial range spacing for processing the surface response is 7.5 mm, which is equivalent to 20 GSample/s.

We simulated a system illuminating a plane surface with different slopes. Therefore a high-resolution range image with 300x300 pixels of the sloped surfaces is calculated to determine the surface response. For surface reflectance a homogenous surface with 100% reflectance was assumed. The distance to the surface center is 100 m.

Examples of the calculated surface response $S[z]$ in dependence of the range z for a slope of 25° received from an uniform beam distribution and a Gaussian beam distribution is shown in Fig. 3a and Fig. 3b. The maximum of the surface response is at the range of 100m.

IV. Overview Of The Experimental Setup

An experimental setup was built up for exploring the capabilities of a laser scanning system, which allows capturing the waveform.

The laser system has three main components: an emitter unit, a motion control unit, and receiver unit.

A. Emitter unit

We use a laser pulse system with a pulse duration of 5 ns at full-width-at-half-maximum (FWHM) and a high repetition rate (42 kHz). The average power of the laser is up to 10 kW. The multi-mode Erbium fiber laser operates at a wavelength of 1550 nm with a beam divergence of 1 mrad and a uniform beam distribution. The transmitted waveform of the emitted pulse shows strong random modulation for each emitted pulse. In Fig. 2 two examples of the transmitted waveform are depicted. The shape of the waveform and the spatial beam distribution depends on the design of the laser system. The system uses a photodiode to pump the multi mode fiber cavity and a fiber amplifier.

B. Motion control unit

For the 2-d scanning process a moving mirror is used for an elevation scan with ±15° in vertical direction (320 raster steps) and a rotation stage for an azimuth scan with 360° rotation in horizontal direction (variable number and spacing of the raster steps).

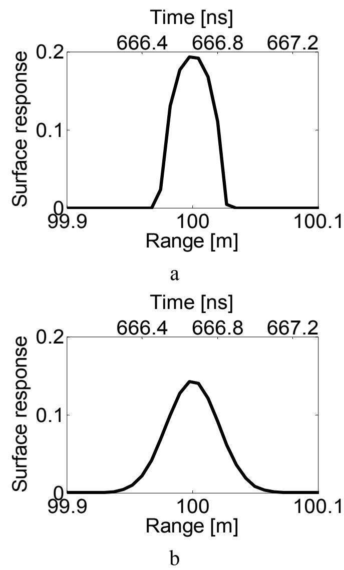

Figure 3. Examples of two surface responses for a slope with 25° and different spatial beam distributions: a) uniform, b) Gaussian.

1-4244-0712-5/07/$20.00 ©2007 IEEE.

C. *Receiver unit*

The receiver unit to capture the waveform contains an InGaAs photodiode with a bandwidth of 1 GHz. Furthermore, we use an A/D converter with 20 GSample/s. The A/D conversion and digital recording is accomplished by using a digital memory oscilloscope (Le Croy - Wavemaster 8600A), where the bandwidth of the oscilloscope is limited to 6 GHz.

V. ESTIMATING THE SLOPE OF A PLANE SURFACE

First the transmitted waveform $s[t]$ and the received waveform $r[t]$ have to be measured with the receiver unit of the laser system. Then by the use of the transmitted waveform and the modeled surface response (Fig. 4-1) for different slopes of the surface the estimated received waveform (Fig. 4-2) can be calculated by a convolution. These estimated received waveforms calculated for different slopes of the plane surface are compared with the measured waveform by determining different normalized cross-correlation functions. With the maximum coefficient of the different normalized cross-correlation functions for different slopes the most likely slope and the accurate range of the surface can be determined (Fig. 4-3). Fig. 4 depicts a schematic description of the processing chain.

The data analysis begins with the detection of the backscattered pulses in the temporal signal. This signal is disturbed by various noise components in form of background radiation, amplifier noise, photo detector noise etc. The detection of the received waveform of the backscattered pulse in noisy data and the extraction of the associated travel time is a well-known problem. It is discussed in detail in radar techniques and system theory [6][7]. Due to this problem the matched filter approach can be used.

To improve the range accuracy and the signal-to-noise ratio the matched filter for the waveform of the backscattered pulse has to be determined. In practice, it is difficult to determine the optimal matched filter. In cases where no optimal matched filter can be determined, sub-optimum filters may be used, but at the cost of decreasing the signal-to-noise ratio. If the temporal deformation of the received waveform can be neglected and the waveform is uniformly attenuated the transmitted waveform of the emitted pulse is the best choice for the matched filter coefficients determination. In practice, the temporal deformation by the surface is common phenomenon. In this paper, we focus on determining this optimal filter by calculating the estimated received waveform.

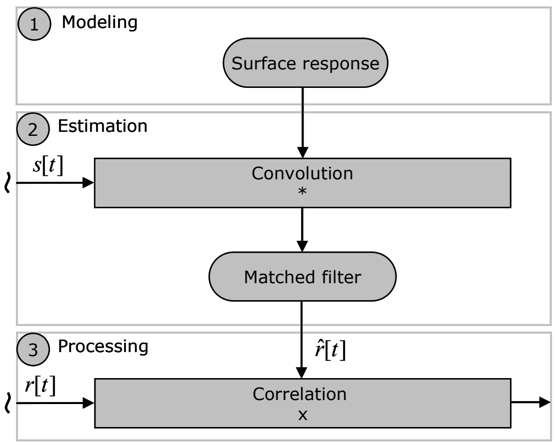

Figure 4. Processing chain to estimate the slope of the surface.

The matched filter is computed by the normalized cross-correlation function $R_{r\hat{r}}$ between the transmitted waveform $s[t]$ of the emitted pulse and the estimated received waveform $\hat{r}[t]$ of the backscattered pulse. A hypothesis for the estimated received waveform $\hat{r}[t]$ is determined by a convolution between the transmitted waveform $r[t]$ and different simulated surface responses $S[z]$, derived by different slopes of the plane surface. A uniform beam distribution is used for processing the different surface responses.

Assuming zero-mean waveforms, we obtain the output signal $R_{r\hat{r}}[\tau]$ with a local maximum at the delay time τ

$$R_{r\hat{r}}[\tau] = \frac{\sum_{t=0}^{M-1} r[t+\tau] \cdot \hat{r}[t]}{\sqrt{\sum_{t=0}^{M-1} r[t]^2 \cdot \sum_{t=0}^{M-1} \hat{r}[t]^2}} \tag{2}$$

where M is the length of the correlation function $R_{r\hat{r}}[\tau]$.

Then the output signal $R_{r\hat{r}}$ is analyzed by a detection filter searching for the local maximum to determine the travel time of the pulse. For each angle φ of the surface the local maximum of the correlation function $R_{r\hat{r}}$ is determined and for the greatest local maximum the most likely slope of the plane surface is estimated.

VI. EXPERIMENTS

An experimental setup with a pulsed multi-mode Erbium fiber laser was built up for exploring the capabilities of waveform analysis for estimating the slope of a plane surface. The transmitted and the received waveforms are captured with an overall bandwidth of 1 GHz. Both analog signals were sampled with a rate of 20 GSample/s.

For the experiments, 500 samples of the transmitted and received waveform derived from a plane plate with different slopes were captured for each angle. The angle φ of the plane surface was changed in steps of 5° from 0° to 60°. The range of the plate to the laser was about 6 m. The footprint diameter at the surface was increased to 25 cm. This footprint diameter is equivalent to a laser scanning system with a beam divergence of 1 mrad at a range of 250 m.

The angle φ of the plane surface with slope was estimated by the greatest maximum for each of the 500 samples. The 3-d histogram in Fig. 5 shows the distribution of the angle for the slope compared with the estimated angles. Further the average value of the estimated angles $\bar{\varphi}$ and the standard deviation σ_φ is depicted in Fig. 6 and the values are listed in Table I.

There is a good similarity between the average value of the estimated angles and the angle of the sloped surface. The average value yields to very good results, except for $\varphi = 0°$.

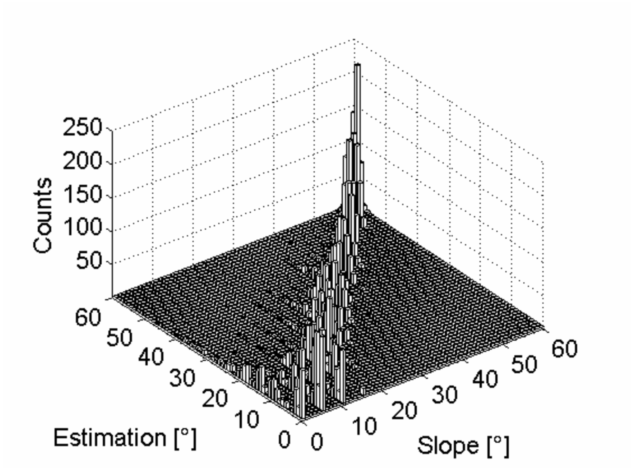

Figure 5. 3d-histogram of the slope compared with the estimated angles.

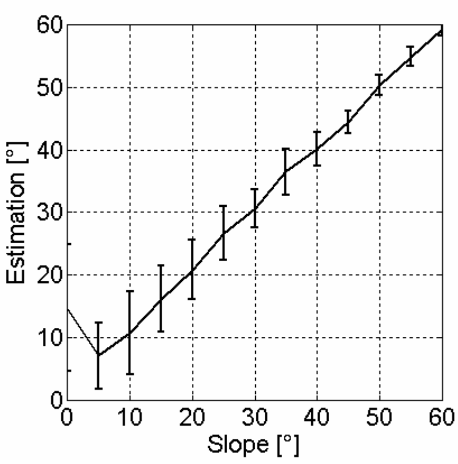

Figure 6. Average and standard deviation of the estimated angle.

For an increasing angle of the sloped surface the standard deviation is decreasing. Low aspect angles show high variation of the angle. The standard deviation for the estimated angles is within the interval $0.99° \le \sigma_{\varphi} \le 10.13°$.

VII. Conclusion

In this work we have presented a scheme to estimate the slope of a plane surface. We simulated the surface response for different slopes and the corresponding received waveform was calculated. The similarity of the estimated and the measured received waveform was used to determine the slope of the surface. It was shown that an accurate estimation is possible, especially for an increasing angle. This could be further improved by considering neighborhood relations. The data generation and analysis we carried out are general investigations for a laser system which records the full-waveform of laser pulses.

TABLE I. Average and standard deviation of the estimated angle.

φ [°]	$\bar{\varphi}$ [°]	σ_{φ} [°]
0	14.67	10.13
5	7.02	5.28
10	10.67	6.68
15	16.15	5.34
20	20.83	4.84
25	26.61	4.32
30	30.65	3.10
35	36.47	3.60
40	40.14	2.71
45	44.47	1.83
50	50.36	1.56
55	54.92	1.55
60	59.34	0.99

References

[1] E.P. Baltsavias, "Airborne laser scanning: existing systems and firms and other resources," ISPRS Journal of Photogrammetry & Remote Sensing 54, pp. 164-198, 1999.

[2] S. Der, B. Redman, R. Chellappa, "Simulation of error in optical radar measurements," Applied Optics 36 (27), pp. 6869-6874, 1997.

[3] M.A. Hofton, J.B. Blair, "Laser altimeter return pulse correlation: A method for detecting surface topographic change," Journal of Geodynamics special issue on laser altimetry 34, pp. 491-502, 2002.

[4] B. Jutzi, U. Stilla, "Laser pulse analysis for reconstruction and classification of urban objects," In: H. Ebner, C. Heipke, H. Mayer, K. Pakzad, Eds. Photogrammetric Image Analysis PIA'03. International Archives of Photogrammetry and Remote Sensing. Vol. 34, Part 3/W8, pp. 151-156, 2003.

[5] B. Jutzi, U. Stilla, "Measuring and processing the waveform of laser pulses," In: A. Gruen, H. Kahmen, Eds. Optical 3-D Measurement Techniques VII. Vol. I, pp. 194-203, 2005.

[6] A. Papoulis, *Probability, Random Variables, and Stochastic Processes*. Tokyo: McGraw-Hill, 1984.

[7] M.I. Skolnik, *Introduction to radar systems*. McGraw-Hill International Editions, Second Edition, 1980.

[8] O. Steinvall, T. Carlsson, "Three-dimensional laser radar modeling," In: G.W. Kamerman, Ed. Laser Radar Technology and Application VI, SPIE Proc. Vol. 4377, pp. 23-34, 2001.

[9] K.H. Thiel, A. Wehr, "Performance Capabilities of Laser-Scanners - An Overview and Measurement Principle Analysis," International Archives of Photogrammetry, Remote Sensing and Spatial Information Sciences 36 (Part 8/W2), pp. 14–18, 2004.

[10] K.H. Thiel, A. Wehr, C. Hug, "A New Algorithm for Processing Fullwave Laser Scanner Data," EARSeL 3D-Remote Sensing Workshop, on CDROM, 2005.

[11] W. Wagner, A. Ullrich, T. Melzer, C. Briese, K. Kraus, "From single-pulse to full-waveform airborne laser scanners: Potential and practical challenges," In: M.O. Altan, Ed. International Archives of Photogrammetry and Remote Sensing. Vol 35, Part B3, pp. 201-206, 2004.

[12] A. Wehr, U. Lohr "Airborne laser scanning – an introduction and overview," ISPRS Journal of Photogrammetry & Remote Sensing 54, pp. 68-82, 1999.